

DOI: 10.13476/j.cnki.nsbdaq.2020.0039

施伟, 成立. 水源地取水泵站水流流态数值模拟与改善[J]. 南水北调与水利科技(中英文), 2020, 18(2): 159-166. SHI W, CHENG L. Numerical simulation and improvement of flow pattern of water intake pumping station in water source area[J]. South-to-North Water Transfers and Water Science & Technology, 2020, 18(2): 159-166. (in Chinese)

水源地取水泵站水流流态数值模拟与改善

施伟^{1,3}, 成立²

(1. 南水北调东线江苏水源有限责任公司, 南京 210019; 2. 扬州大学 水利科学与工程学院, 江苏 扬州 225000;
3. 江苏省泵站工程技术中心, 南京 210019)

摘要:为解决取水泵站预沉池内水流流态紊乱、曝气池及前池存在大面积回流区及旋涡等问题, 针对某一具体水源地取水泵站, 基于三维不可压缩流体的有限体积法和标准 $k-\epsilon$ 湍流模型, 采用 ANSYS CFX 软件对该泵站预沉池、曝气池及前池进行数值模拟计算。通过对计算结果进行后处理, 分析了取水泵站所选横断面水流流态、流速云图以及压力云图。在原方案基础上通过对曝气池廊道转角处设置倒圆角、廊道转角内设置“U”形导流墙与 1/4 弧形导流墙、前池内设置八字形导流墩及泵机组间设隔墩来对泵站进行优化。优化后改进方案与原方案相比, 廊道转角处脱流、回流现象得到改善, 曝气池及前池内大范围回流区域消失, 泵站整体水流不存在明显的不良流态。该研究成果对于优化内水流流态, 预防泥沙沉淀, 提高泵站运行稳定性、高效性、安全性有一定的指导意义。

关键词:取水泵站; 预沉池; 曝气池; 前池; 流态; 数值模拟

中图分类号: TV671; TV131 文献标志码: A 开放科学(资源服务)标识码(OSID):



我国水资源总量匮乏且水资源地区分布不均, 为使水资源短缺等问题有效地减缓和解决, 跨流域调水工程的科学调度、优化运行显得尤为迫切与必要^[1-3]。随着我国现代化建设的不断加快, 国内调水工程也发展十分迅速, 针对调水工程中水力优化等问题, 国内专家学者进行了广泛研究。预沉池、曝气池及前池为调水工程中取水泵站主要构筑物, 预沉池的作用主要是去除水中的可沉物和漂浮物, 若预沉池内水流紊乱, 则不利于泥沙沉降, 可能会造成曝气池及前池的泥沙淤积^[4-5]。魏文礼等^[6]基于两相流模型对沉淀池内水力特性展开研究, 该模型可较准确的模拟出沉淀池内流场的分布情况; 白玉华等^[7]对沉淀池内水流流态进行数值模拟与优化; 刘天杰等^[8]基于标准 $k-\epsilon$ 紊流模型, 对不同进水条件下, 模拟了沉淀池内部水流流态及固体颗粒悬浮物浓度分布; 王晓玲等^[9]基于建立的平流式沉淀池两

相流模型, 采用 STAR-CD 数模软件对沉淀池内流场进行求解计算, 同时考虑悬浮物浓度及固液两相密度差的影响, 研究回流区、沉淀区流速分布及湍流动能; 苏军伟等^[10]阐述并分析了影响二沉池内两相流动精确模拟的污泥沉降速度、混合液流变性质、外界风场、二沉池结构等因素。

曝气池主要是利用活性污泥法进行污水处理, 但因为廊道较长, 容易出现明显的脱流及大面积死水区现象, 对取水泵站整体水流流态产生不利影响^[11-12]。程文等^[13]对曝气池中气液两相流流动规律进行了实验研究, 对曝气池内的液相的垂向速度进行了测量。王蒙等^[14]采用实验研究与数值模拟相结合的方法, 对圆柱形气液装置进行 PIV 实验, 获得了准确的气液两相流相速度场分布, 提出的欧拉-欧拉双流体模型和气泡群平衡模型模拟方法在气液两相流模拟中能够得到较准确的两相流动规

收稿日期: 2019-09-02 修回日期: 2019-12-17 网络出版时间: 2019-12-19

网络出版地址: <http://kns.cnki.net/kcms/detail/13.1334.TV.20191219.1616.008.html>

基金项目: 国家自然科学基金(51779214); 江苏省第五期“333 高层次人才培养工程”(BRA2018382); 江苏省工信厅 2018 年度第二批省级工业和信息产业转型升级专项资金

作者简介: 施伟(1980—), 男, 江苏盐城人, 高级工程师, 博士研究生, 主要从事泵站工程建设与管理。E-mail: nsbdsw@126.com

律和速度场分布情况。

前池大部分情况下采用扩散入流方式,但由于实际工程中前池扩散段较短,水流难以得到充分扩散,极易在前池形成较大面积的回流区,影响水泵机组的安全运行。罗灿等^[15]基于 N-S 方程,对正向进水的前池流态进行研究改善;高传昌等^[16-17]通过试验对前池流态进行研究,通过设置挑流墩、压水板等措施后,前池内流态得到改善;成立等^[18-19]通过改变底坎形式,研究不同底坎形式绕流流速分布情况及底坎位置的选择。冯建刚^[20]、周龙才^[21]、印超^[22]及刘超^[23]等人对泵站前池内流场进行数值模拟,研究增设措施后流场分布规律并提出相应的整流措施。

随着跨流域调水工程的深入开展,对取水泵站预沉曝气池及前池水流流态改善的研究显得极为迫切。因此,本文基于某市新水源地取水泵站整体,采用 CFD(computational fluid dynamics)技术,软件使用 ANSYS 14.5 进行计算,紊流模型选取标准 k-ε 紊流模型。计算不同流量不同水位工况下的优化方案以及原方案,通过两个流程图、速度云图及压力云图的比较,分析优化措施对原方案水流流态的改善情况。

1 工程概况

本文引用的泵站为某市新水源地取水泵站,取

水泵房内设 10 台泵位,水泵根据各种工况灵活搭配。设 7 台高扬程水泵,5 用 2 备,单泵流量 $2.875 \text{ m}^3/\text{s}$,扬程 58.5 m,功率 2 240 kW,全变频;设 3 台低扬程水泵,3 全用,单泵流量 $2.551 \text{ m}^3/\text{s}$,扬程 29 m,功率 1 000 kW,全变频。以大泵变频作为小泵的备用。

泵站大流量工况下流量为 $13.31 \text{ m}^3/\text{s}$ 、扬程为 58.5 m,小流量工况下流量为 $7.80 \text{ m}^3/\text{s}$ 、扬程为 40.5 m,泵站设计高水位为 6.8 m、设计常水位为 3.9 m、设计低水位为 2.4 m。

2 数值模拟计算

2.1 流体动力学方程及紊流模型

取水泵站内部流动为不可压缩湍流流动,该流动可用雷诺时均 N-S 流体动力学基本方程和连续性方程来描述,同时本文选取适用范围较为广泛标准 k-ε 紊流模型进行计算^[24-25]。

2.2 网格划分

本文对取水泵站预沉池、曝气池及前池分别进行网格划分,利用商用软件 ANSYS 14.5 中的 mesh 软件进行划分,采用分块策略,见图 1,将取水泵站整体分为 9 个部分,分别是穿孔花墙及两侧进水部分、左右预沉淀池、曝气池廊道及斜坡段、前池部分、出水段。

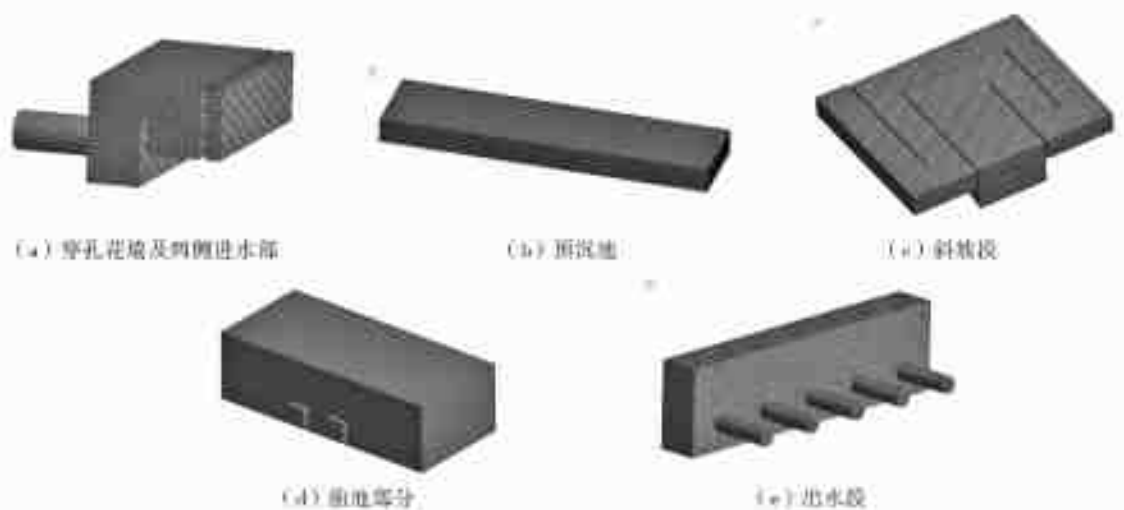


图 1 计算域网格分块划分

2.3 网格无关性分析

计算域网格数量级的选取以及网格质量的优劣对于本文研究取水泵站的整体水流动特性尤为重要,因此,对取水泵站整体进行了网格无关性分析。在 40 万至 240 万内任意选取 9 个控制网格数并进行网格无关性分析。选取 1-1 断面(泵站进口)和 2-2 断面(泵站出口)间的水力损失进行水力损失计

算,如图 2 所示。



图 2 数值模拟计算区域

图 3 为取水泵站不同网格数量下的网格无关性分析,以取水泵站整体水力损失为指标,随着网格数的增加,水力损失逐步上升,当网格数量大于 150 万

时,水力损失趋于稳定,无明显变化。理论上,计算结果的精确程度取决于网格数的多少,而过多的网格数,会大量耗费计算数值时间,造成计算机资源的浪费。最终计算域整体网格数量为 175.6 万个,整个计算域网格节点数为 172.6 万个。

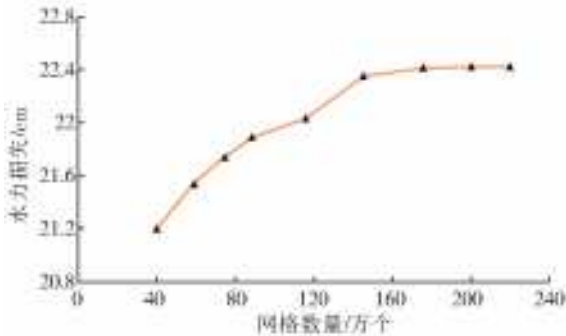


图3 不同网格数下取水泵站水力损失

3 计算方案及结果

3.1 计算方案

水流通过斜坡以闸孔入流方式进入前池,由于水流主流集中且流速较快,主流在短时间内无法均匀扩散进入各泵站机组,在前池内两侧易形成了大面积同向旋转的旋涡,不利于泵机组安全稳定运行。根据某地新水源地取水泵站的设计图纸,建立曝气池的三维模型。原方案模型见图4。针对廊道内存在的脱流、死水区,在原方案的基础上加设倒圆角,在廊道内增设“U”形导流墙与1/4弧形导流墙;针对斜坡段偏流及回流旋涡,在原方案前池设“八字形”导流墙,并在泵站机组之间加设导流墩,可使水流相对平顺地进入前池。改进方案模型见图5。

3.2 计算结果

为了解不同方案在不同水位和流量条件下取水



图4 原方案模型

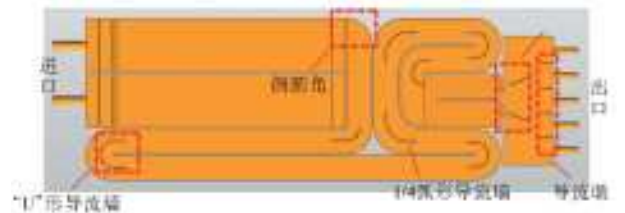


图5 改进方案模型

泵站内水流流动特性,对两个特殊工况点(小流量 $Q=7.80 \text{ m}^3/\text{s}$ 、大流量工况 $Q=13.31 \text{ m}^3/\text{s}$)及三个特殊水位(设计低水位 2.4 m、设计常水位 3.9 m、设计高水位 6.8 m)下不同取水泵站方案的内部水流流动特性进行数值模拟计算。选取取水泵站中高度为 1 m 的断面($Z=1 \text{ m}$)作为分析断面,通过后处理得到取水泵站流线图、流速云图、压力云图进行对比分析。

3.2.1 不同方案取水泵站整体流线图分析

通过对不同工况及水位条件下两个方案的取水泵站流场模拟计算发现,由流线图6—图8可知,原方案沉淀区水流流态较为平顺,但在廊道的转角处存在小旋涡、流态较为紊乱,而在前池的左侧存在大面积旋涡、回流区。而在改进方案内廊道转角处脱流、回流得到改善,流线分布更加均匀。在低水位工况条件下,前池左侧大回流区得以消除,整体水流不存在明显的不良流态;在常水位及高水位工况条件下,前池虽存在旋涡,但廊道与斜坡段的脱流、回流现象得到改善。

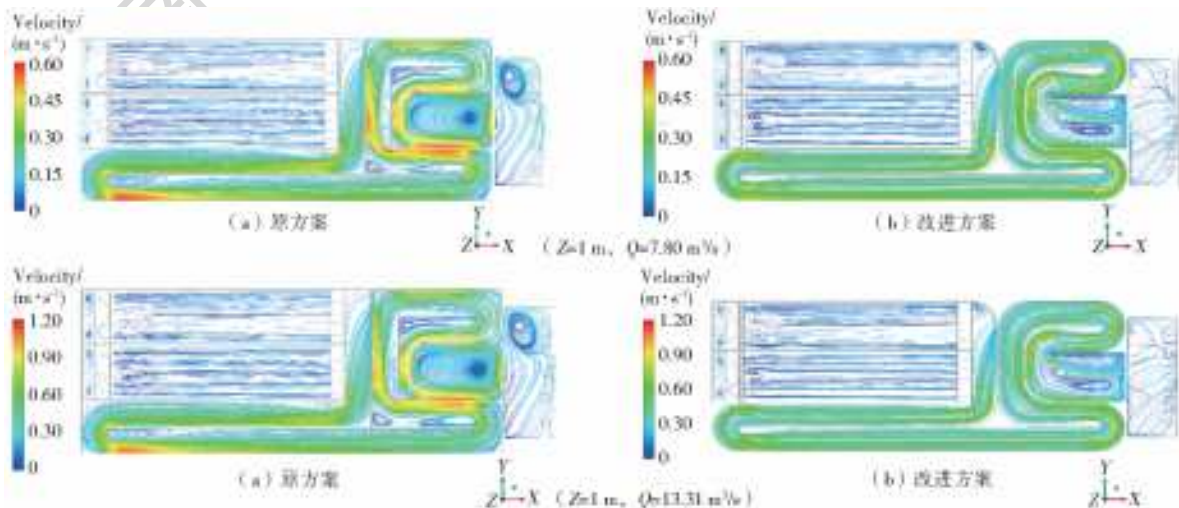


图6 不同流量工况下原方案与改进方案低水位流线

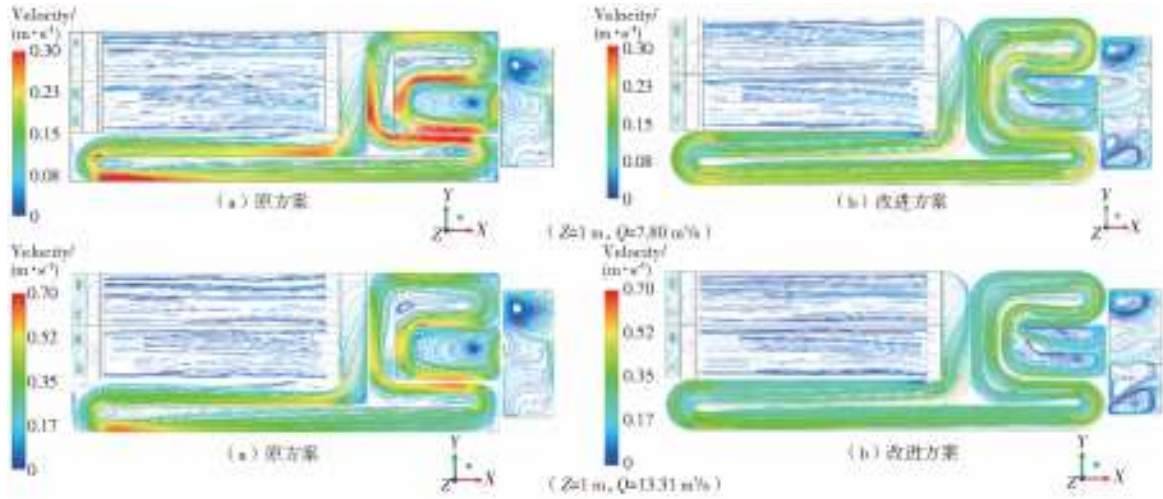


图 7 不同流量工况下原方案与改进方案常水位流线

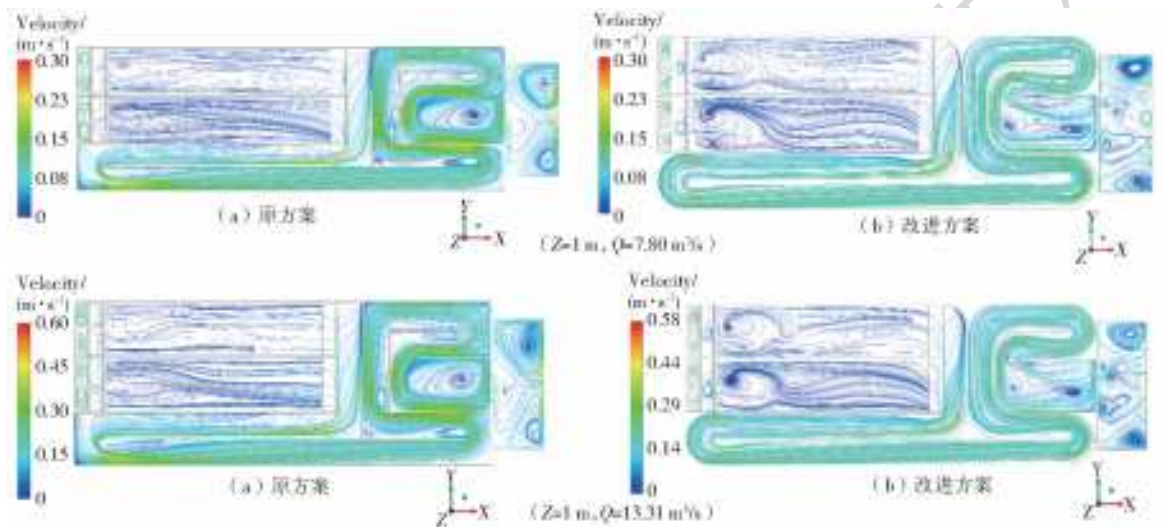


图 8 不同流量工况下原方案与改进方案高水位流线

取水泵站内当水位一定时,随着流量的增加,两个方案流线变化较小,而原方案与改进方案之间流线的对比变化规律与流量无关。

当流量一定、水位抬升至常水位、高水位时,两个方案整体水流流态与低水位时相比变化较小,改

进方案对原方案存在的不良流态的改善较明显。

3.2.2 不同方案取水泵站整体流速云图分析

通过对不同工况及水位条件下两个方案的取水泵站内部流场模拟计算发现,由流速云图 9—图 11 可知,原方案在廊道转角处存在高速区,流速分布不

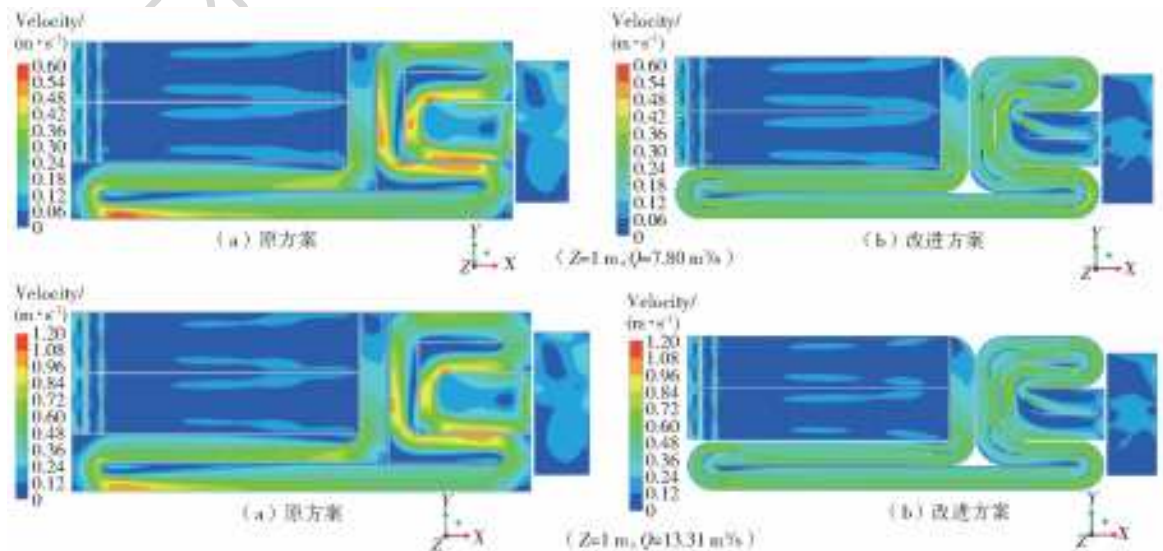


图 9 不同流量工况下原方案与改进方案低水位流速云图

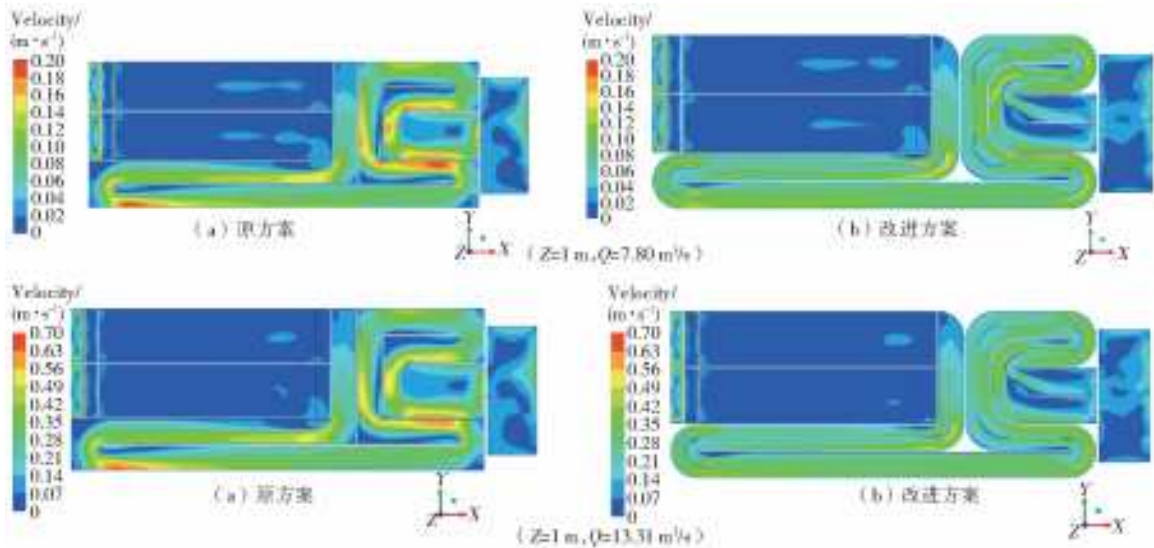


图 10 不同流量工况下原方案与改进方案常水位流速云图

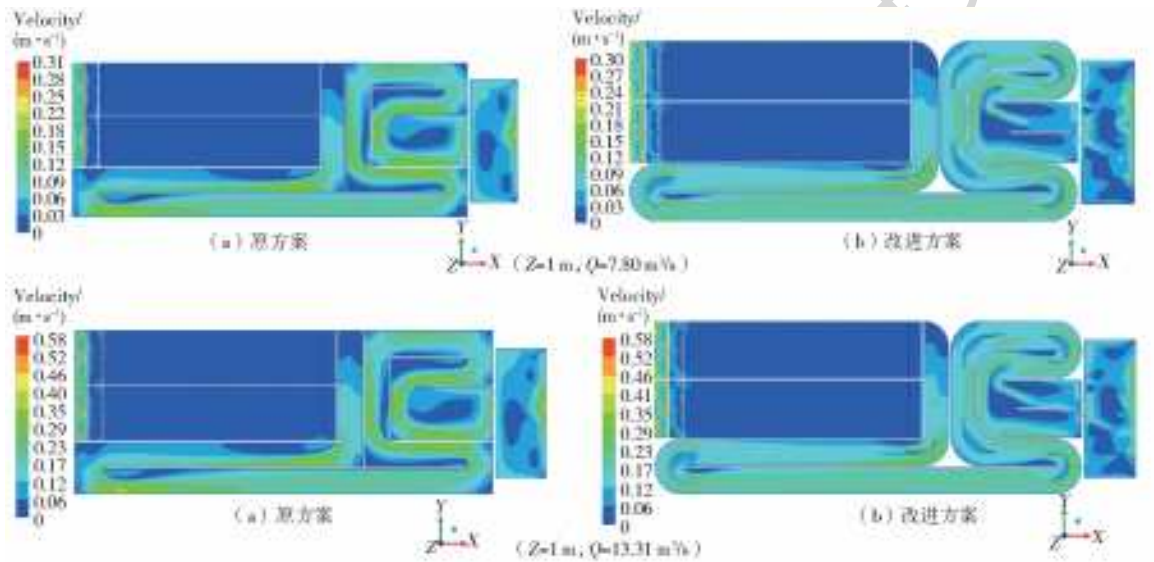


图 11 不同流量工况下原方案与改进方案高水位流速云图

均匀,前池内流速分布也不均匀。而在改进方案内整体水流流速分布较为均匀,不存在明显的流速波动,廊道转角处的流速分布不均匀得到改善。

取水泵站内当水位一定时,随着流量的增加,两个方案整体流速逐渐增大但变化规律类似,而原方案与改进方案之间流速的对比变化规律与流量无关。

当流量一定、水位抬升至常水位、高水位时,由流速云图可知,常水位和高水位的两个方案内的流速和低水位时相比减小,流速分布基本不变,改进方案使取水泵站整体流速分布更加均匀。

3.2.3 不同方案取水泵站整体压力云图分析

通过对不同工况及水位条件下两个方案的取水泵站流场模拟计算发现,由压力云图 12—14 可知,改进方案与原方案相比较,廊道内压力较小,压力分布更加均匀。

取水泵站内当水位一定时,随着流量的增加,整体压力数值逐渐增大但变化规律类似,而原方案与改进方案之间压力的对比变化规律与流量无关。

当流量一定、水位抬升至常水位、高水位时,与低水位时相比,两个方案整体压力数值减小,但压力分布大致相同,改进方案压力分布均匀度比原方案更佳。

3.3 计算结果分析

为了定量分析比较两种流量工况下原方案与改进方案各水泵机组吸水均匀性的差异,对 5 台水泵机组(图 15)喇叭管入口断面流速均匀度进行对比分析。

特征断面流速均匀度的计算公式为

$$\bar{V}_u = \left[1 - \frac{1}{u_a} \sqrt{\frac{\sum (u_{ai} - \bar{u}_a)^2}{m}} \right] \times 100\%$$

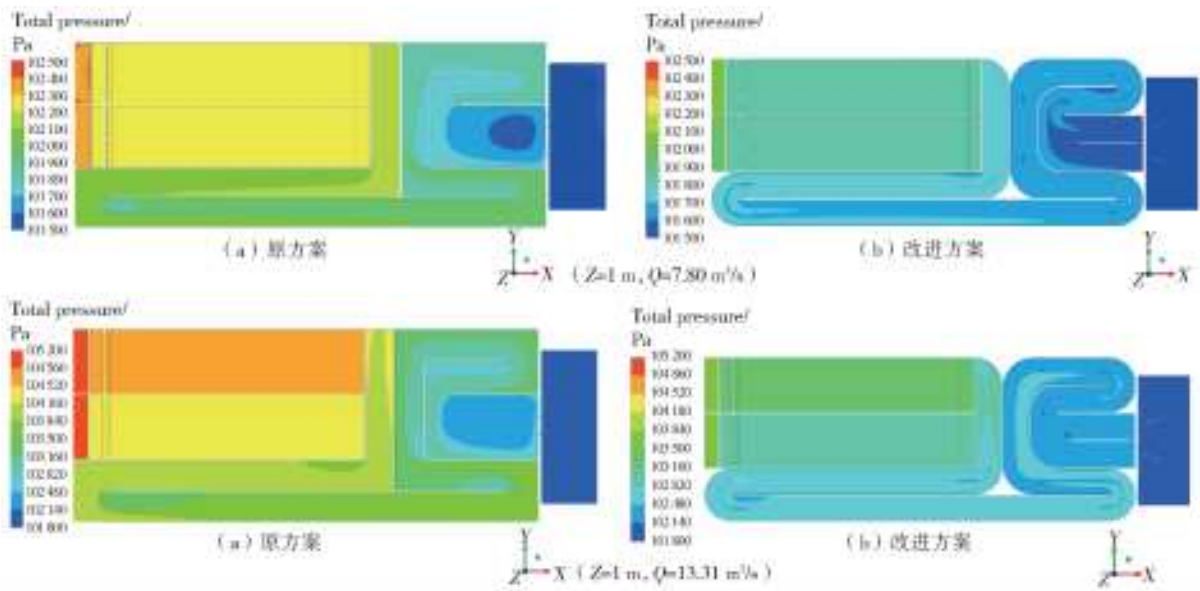


图 12 不同流量工况下原方案与改进方案低水位压力云图

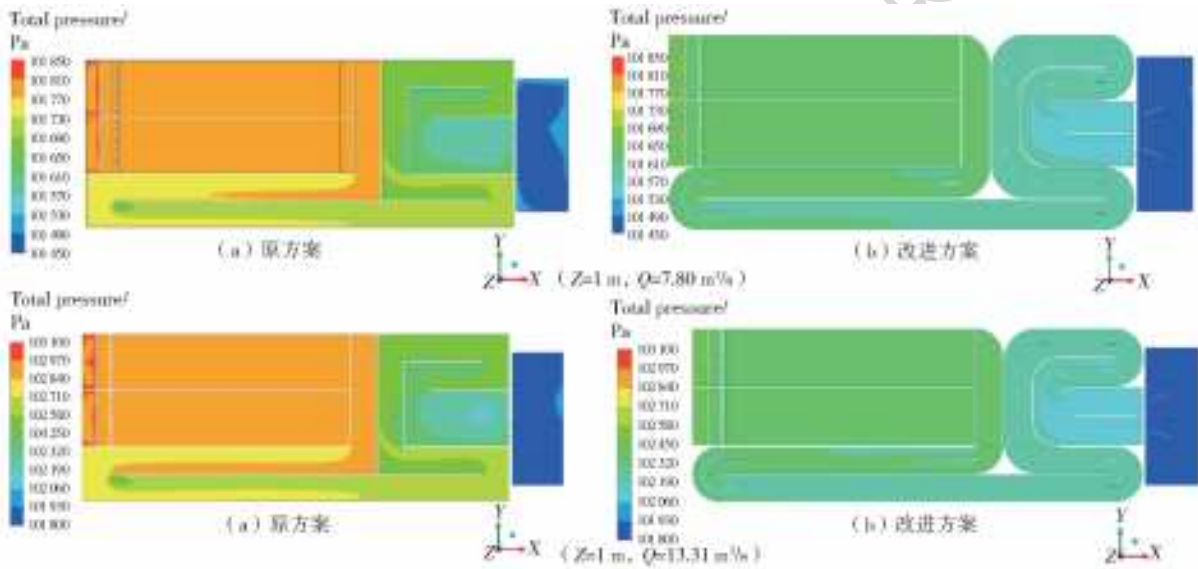


图 13 不同流量工况下原方案与改进方案常水位压力云图

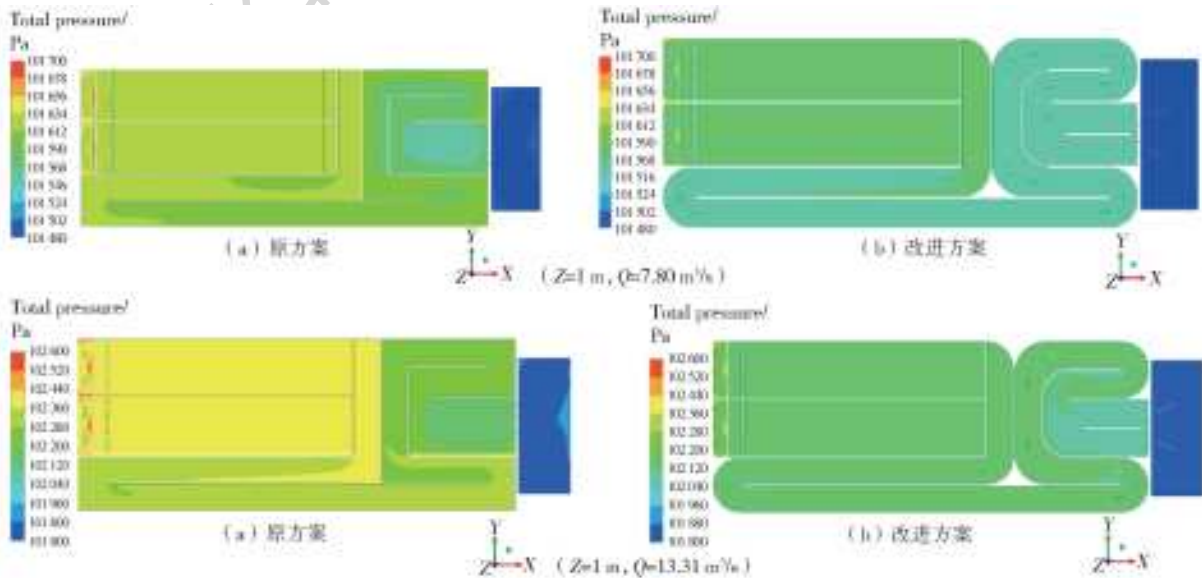


图 14 不同流量工况下原方案与改进方案高水位压力云图

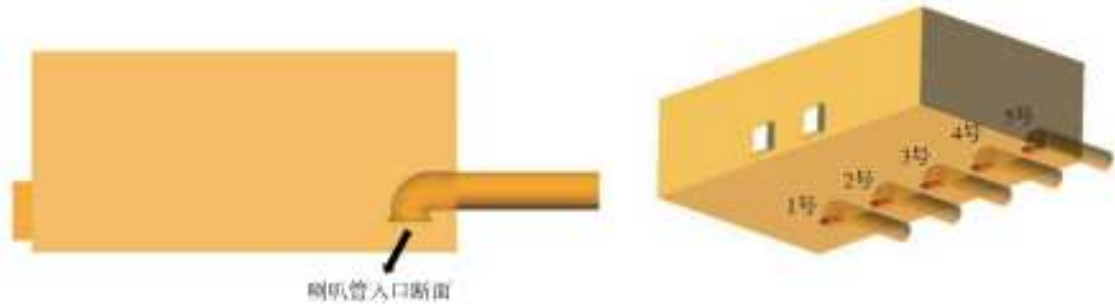


图 15 泵机组编号

式中: \bar{u}_a 为垂直特征断面的平均轴向速度,m/s; u_{ai} 为垂直特征断面第*i*个单元轴向速度,m/s; m 为断面网格单元数。

图 16 为两种流量工况下喇叭管各入口断面流速均匀度。计算结果表明:两种流量工况下未添加改善措施的前池各水泵吸水均匀性差异均较大,两侧水泵吸水均匀性较差。通过在前池加设倒圆角,

廊道内增设“U”形导流墙以及在前池设八字形导流墙,泵站之间加设导流墩后,5 台水泵在两种流量工况下的吸水均匀性均得到显著提高,喇叭管入口断面流速均匀度最大提高幅度达 3.6%,且各泵机组喇叭管入口断面最大流速均匀度差异缩小至 1.8%以内,但靠近前池两侧泵机组吸水均匀性相比中间 3 台机组吸水均匀度较差。

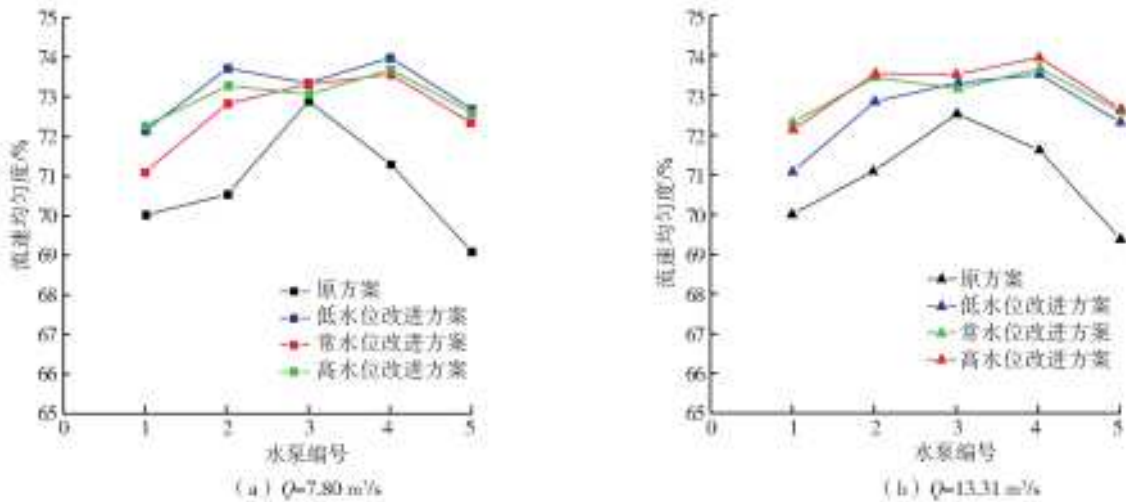


图 16 不同流量工况下喇叭管各入口断面流速均匀度

4 结 语

(1) 取水站在原方案的基础上对曝气池廊道转角处设置倒圆角、廊道转角内设置“U”形导流墙与 1/4 弧形导流墙、前池内设置八字形导流墩及泵机组间设隔墩。原方案沉淀区水流流态较为平顺,但在廊道的转角处存在小漩涡、流态较为紊乱,而在前池的左侧存在大面积漩涡、回流区。而在改进方案内廊道转角处脱流、回流得到改善,流线分布更加均匀,且水泵喇叭管各入口断面流速均匀度有较大提升。尤其在低水位工况条件下,前池左侧大回流区得以消除,整体水流不存在明显的不良流态。

(2) 取水站前池无整流措施时,斜坡闸孔入流后,后壁受射流形式水流撞击,极易在两侧形成大面积的回流区。通过在前池内两闸孔中线处设置八字

形导流墩及泵机组间设隔墩,较好地控制了低水位工况条件下的面层大面积回旋区。

(3) 当取水站内水位一定时,随着流量的增加,流线变化不大,整体流速和压力逐渐增大但变化规律类似,而原方案与改进方案之间流线、流速以及压力的对比变化规律与流量无关。当流量一定、随着水位的抬升,整体水流流态与低水位时相比变化较小,改进方案对原方案存在的不良流态改善较明显,水泵吸水均匀性得到显著提高。流速相对减小但流速分布基本不变,整体压力数值减小,但压力分布大致相同,沉淀区水流流态变差。

参考文献:

- [1] 刘超. 水泵及水泵站[M]. 北京: 中国水利水电出版社, 2009.

- [2] 成立,刘超,颜红勤,等. 泵站水流运动特性及水力性能[M]. 北京:中国水利水电出版社,2016.
- [3] 李浩,黄薇,刘陶,等. 跨流域调水生态补偿机制探讨[J]. 自然资源学报,2011,26(9):1506-1512. DOI:10.11849/zrzyxb. 2011. 09. 006.
- [4] 朱维轩,田宝义,李辰. 南水北调西河水源预沉池流场分布模拟及优化[J]. 中国给水排水,2014,30(9):63-65.
- [5] 王金山,王志强. 包头市磴口水厂旋流式预沉池工艺设计研究[J]. 内蒙古科技与经济,2005(1):94-95. DOI:10.3969/j. issn. 1007-6921. 2005. 01. 040.
- [6] 魏文礼,张沛,刘玉玲. 平流式沉淀池水力特性三维数值模拟[J]. 沈阳农业大学学报,2014,45(4):499-502. DOI:10.3969/j. issn. 1000-1700. 2014. 04. 023.
- [7] 白玉华,李琳,柳藤,等. 基于 LDV 测速考察风速风向对平流式沉淀池水流运动的影响[J]. 西南给排水,2014,36(4):14-20.
- [8] 刘天杰,胡润麟,孙泽,等. 平流式沉淀池穿孔墙进水及隔板作用数值模拟[J]. 供水技术,2015,9(4):1-6. DOI:10.3969/j. issn. 1673-9353. 2015. 04. 001.
- [9] 王晓玲,杨丽丽,张明星,等. 平流式沉淀池水流三维 CFD 模拟[J]. 天津大学学报,2007(8):921-930. DOI:10.3969/j. issn. 0493-2137. 2007. 08. 008.
- [10] 苏军伟,王乐,陈杰. 二沉池数值模拟研究的综述与评论[J]. 环境工程,2019,37(4):87-92. DOI:10.13205/j. hjgc. 201904017.
- [11] 肖柏青,张法星,戎贵文. 气泡尺寸对曝气池内气液两相流数值模拟的影响[J]. 中国环境科学,2012,32(11):2006-2010. DOI:10.3969/j. issn. 1000-6923. 2012. 11. 012.
- [12] 刘玉玲,白戈,邵世鹏,等. 曝气池曝气管布置方式对流速分布影响的数值模拟研究[J]. 水力发电学报,2016,35(7):84-90. DOI:10.11660/slfdb. 20160709.
- [13] 程文,宋策,周孝德. 曝气池中气液两相流的数值模拟与实验研究[J]. 水利学报. 2001,44(12):42-45. DOI:10.3321/j. issn:0559-9350. 2001. 12. 006
- [14] 王蒙,孙楠,王颖,等. 曝气池中气液两相流速度场分布的实验研究与数值模拟. 水利学报,2016,47(10):1322-1331. DOI:10.13243/j. cnki. slxb. 20160530.
- [15] 罗灿,成立,刘超. 泵站正向进水前池底坎整流机理数值模拟[J]. 排灌机械工程学报,2014,32(5):393-398. DOI:10.3969/j. issn. 1674-8530. 13. 0122.
- [16] 高传昌,刘新阳,石礼文,等. 泵站前池与进水池整流方案数值模拟[J]. 水力发电学报,2011,30(2):54-59.
- [17] 高传昌,王玉川,石礼文,等. 泵站前池非连续挑流消能防沙技术措施[J]. 排灌机械工程学报,2011,29(2):133-138. DOI:10.3969/j. issn. 1674-8530. 2011. 02. 009.
- [18] 成立,刘超,周济人,等. 水泵站底坎二维绕流湍流数值模拟[J]. 农业机械学报,2005(3):37-39. DOI:10.3969/j. issn. 1000-1298. 2005. 03. 011.
- [19] 成立,刘超,周济人,等. 泵站前池底坎整流数值模拟研究[J]. 河海大学学报(自然科学版),2001(3):42-45. DOI:10.3321/j. issn:1000-1980. 2001. 03. 009.
- [20] 冯建刚,李杰. 大型城市水源泵站前池流态及改善措施试验[J]. 水利水电科技进展,2010,30(2):70-74. DOI:10.3880/j. issn. 1006-7647. 2010. 02. 018.
- [21] 周龙才. 泵站前池隔墩整流的数值分析[J]. 长江科学院院报,2010,27(2):31-33. DOI:10.3969/j. issn. 1001-5485. 2010. 02. 007.
- [22] 印超. 泵站前池流态改善三维数值模拟研究[D]. 扬州:扬州大学,2007.
- [23] 刘超,成立,汤方平. 水泵站前池三维流动计算和试验[J]. 农业机械学报,2001(6):41-44. DOI:10.3969/j. issn. 1000-1298. 2001. 06. 012.
- [24] 王福军. 流体机械旋转湍流计算模型研究进展[J]. 农业机械学报,2016,47(2):1-14. DOI:10.6041/j. issn. 1000-1298. 2016. 02. 001.
- [25] 王伟,张扬,陈利丽. 带有剪切应力输运性质的 k-ε 两方程湍流模型构造与应用[J]. 空气动力学学报,2019,37(3):419-425. DOI:10.7638/kqdlxxb-2016. 0158.

• 译文(Translation) •

DOI:10.13476/j.cnki.nsbdcqk.2020.0039

Numerical simulation and improvement of flow pattern of water intake pumping station in water source area

SHI Wei^{1,3}, CHENG Li²

- (1. The Eastern Route of South-to-North Water Diversion Project Jiangsu Water Source Co, Ltd, Nanjing 210019, China;
2. School of hydraulic Science & Engineering, Yangzhou University, Yangzhou 225009, China;
3. Jiangsu Engineering and Technology Center for Pumping Station, Nanjing 210019, China)

Abstract: In order to solve the problems of turbulent flow pattern in pre-sedimentation tank of intake pumping station, large area of reflux zone and vortices in aeration tank and forebay. Based on the finite volume method of three-dimensional incompressible fluid and standard k- ϵ turbulence model, the numerical simulation of pre-sedimentation tank, aeration tank and forebay of an intake pumping station was carried out by using ANSYS CFX software. The aeration tank and forebay are numerically simulated, and the flow pattern, velocity and pressure contour of the selected cross-section of the intake pumping station are analyzed. The pumping station is optimized by setting fillets at the corridor corner of the aeration tank, U-shaped diversion wall and quarter arc diversion wall in the corridor corner of the original scheme. Splayed diversion piers are set in the forebay and diversion piers are set between pump units. Compared with the original scheme, the phenomenon of flow separation and reflux in the corridor corner of the original scheme has been improved. The large-scale reflux area in the aeration tank and the forebay disappears, and there is no obvious bad flow pattern in the overall flow of pumping station. The research results have certain guiding significance for optimizing the internal water flow, preventing sediment sedimentation, and improving the stability, efficiency and safety of pumping stations.

Key words: intake pumping station; pre-sedimentation tank; aeration tank; forebay; flow pattern; numerical simulation

The total amount of water resources in China is deficient and the distribution of water resources is uneven. In order to effectively solve the water shortage and other problems, it is very urgent and necessary to scientifically dispatch and optimize the operation of inter-basin water transfer project^[1-3]. With the continuous acceleration of China's modernization, the development of water transfer project is also very rapid. In recent years, domestic experts and scholars have conducted extensive research on issues such as hydraulic optimization in

water transfer projects. The pre-sedimentation tank, aeration tank and forebay are the main structures of the water intake pump station in the water transfer project. The role of the pre sedimentation tank is mainly to remove the sinkable and floating objects in the water. If the water flow in the pre-sedimentation tank is turbulent, it will not be conducive to sedimentation, and it may also cause sedimentation in the aeration tank and the forebay^[4-5]. Wei et al^[6] used the gas-liquid two-phase flow model to simulate the 3D hydraulic characteristics

Received: 2019-09-02 Revised: 2019-12-17 Online publishing: 2019-12-19

Online publishing address: <http://kns.cnki.net/kcms/detail/13.1334.TV.20191219.1616.008.html>

Author brief: SHI Wei (1980-), senior engineer, mainly engaged in the pump station engineering construction and management research.
E-mail: nsbdsw@126.com

of a secondary sedimentation tank. The results indicated that the model can well simulate the distribution of hydraulic characteristics in a secondary sedimentation tank. Bai et al^[7] carried out numerical simulation and optimization of flow pattern in sedimentation tank. Based on the standard $k-\epsilon$ turbulence model, Liu et al^[8] simulated the flow pattern and the concentration distribution of solid particles in the sedimentation tank under different inflow conditions. Based on the 3D two-phase flow model, Wang et al^[9] simulated the flow fields in rectangular sedimentation tanks by the computational fluid dynamics software STAR-CD. The interfacial forces as well as the volume fraction of suspended solids and density between suspended solids and liquid were considered in modeling. Su et al^[10] discussed and analyzed the sludge settlement velocity, the rheological properties of mixed liquid, the external wind field and the secondary settling tank structure and other factors affecting the accurate simulation of the two-phase flow dynamics affecting the accurate simulation of the two-phase flow dynamics.

The aeration tank mainly uses the activated sludge process for sewage treatment. Due to the long corridor of the aeration tank, obvious aeration and large-area dead water phenomenon are likely to occur in the aeration tank, which adversely affects the overall flow pattern of the intake pumping station^[11-12]. Cheng^[13] conducted an experimental study on the flow law of gas-liquid two-phase flow in the aeration tank, and measured the vertical velocity of the liquid phase in the aeration tank. Wang^[14] carried a PIV experimental study of gas-liquid two-phase flow on a cylindrical experimental device, and the gas velocity vector fields were obtained accurately by image processing and particle image velocimetry technology.

In most cases, diffusion inflow mode is used in forebay to ensure smooth diffusion of water flow. Due to the short length of the diffusion section in the forebay, the water flow is difficult to be fully diffused, and it is easy to form a large area of reflux

area in the forebay, which affects the safe operation of the pumping system. In order to study the bad flow pattern in the forebay, Luo et al^[15] simulated the flow pattern in the forebay without any measures and with bottom sill rectification measures based on the $N-S$ equation. Gao et al^[16-17] studied the flow pattern in the forebay through experiments, and the results showed that the flow pattern in the forebay was improved after setting the measures such as the trajectory bucket piers and pressure plates.

With the development of the inter-basin water transfer project, it is very urgent to study the improvement of the flow pattern in the pre-sedimentation aeration tank and forebay of the intake pumping station. Hence, based on CFD (computational fluid dynamics) technology, ANSYS 14.5 software was used to carry out numerical simulation of the pre settling aeration tank and forebay of a new water source pumping station in a city, and the standard $k-\epsilon$ turbulence model is selected for the turbulence model. By comparing the internal flow characteristics of the improved schemes and original scheme under different flow rate and water level conditions, the improvement of the flow pattern of the original scheme by the optimization measures was analyzed.

1 Project Overview

The pumping station studied in this paper is the intake pumping station in a new water source area of a city. There are 10 pumps in the pumping house, which can be flexibly matched according to various working conditions. Of the 10 pumps, 7 are high head pumps and 3 are low head pumps. The design flow rate of single high head pump is 2.875 m^3/s , and the design head is 58.5 m. The design flow rate of single low head pump is 2.551 m^3/s , and the design head is 29.0 m.

Under the condition of large flow rate, the flow rate of intake pumping station is 13.31 m^3/s and the head is 58.5 m. Under the condition of small flow rate, the flow rate of intake pumping station is 7.80 m^3/s and the head is 40.5 m. The

design high water level of the pump station is 6.8 m, the design normal water level is 3.9 m and the design low water level is 2.4 m.

2 Numerical Simulation

2.1 Control equations and Turbulence Mode^[24-25]

Reynolds-averaged *N-S* equation and continuity equation were selected to describe the 3D incompressible viscous flow in the intake pumping station. At the same time, the standard *k-ε* turbulence

model was selected for calculation.

2.2 Mesh generation

The Mesh in ANSYS 14.5 software was used to generate grids of pre-sedimentation tank, aeration tank and forebay in the intake pumping station separately. As shown in Fig. 1, the intake pumping station was divided into nine parts for grid generation. The grids of whole computational domain are mainly composed of hexahedral grids.

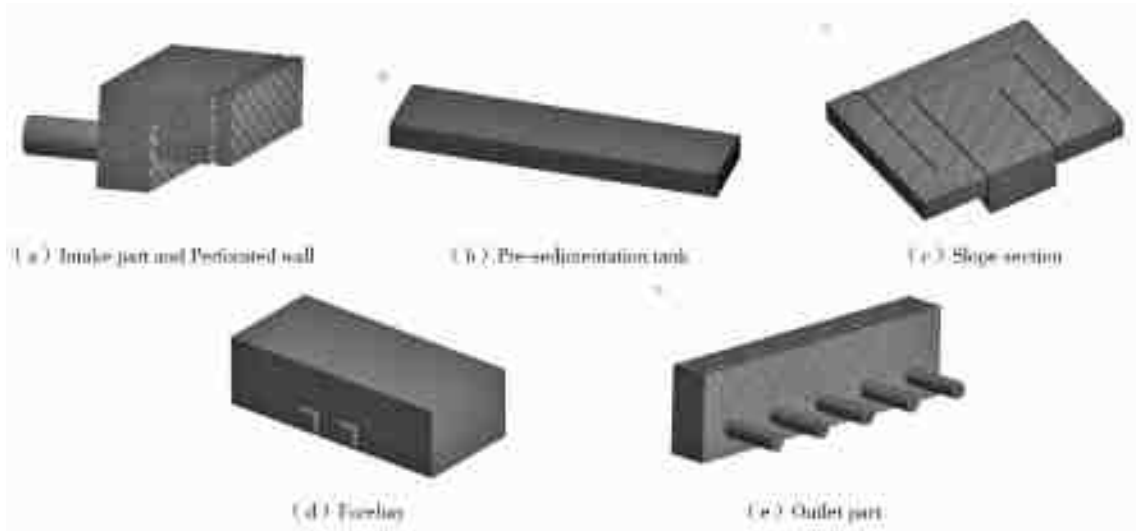


Fig. 1 Mesh of the computation domin

2.3 Mesh independence

It is very important for the accuracy of numerical simulation to select the quantity and quality of the grid. Hence, in order to verify the reasonableness of the mesh generation, the grid independence of the intake pumping station was carried out. In the range of 400 000 to 2 400 000 grid numbers, 9 groups of grid numbers were selected for grid independence analysis to determine the appropriate grid numbers. As shown in Fig. 2, section 1-1 (pumping station inlet) and section 2-2 (pumping station outlet) were selected as the pressure measuring section for hydraulic loss calculation.



Fig. 2 Computation domain

Fig. 3 shows the change of hydraulic loss under different grid numbers of intake pumping station. As shown in the figure, with the increase of

the number of grids, the hydraulic loss increases gradually. When the number of grids is more than 1.5 million, the hydraulic loss tends to be stable without obvious change. Theoretically, the accuracy of the calculation results depends on the number of grids, but too many grids will consume a lot of calculation time, resulting in a waste of computer resources. Finally, the grid number of the entire computational domain is 1.756 million, and the number of nodes is 1.726 million.

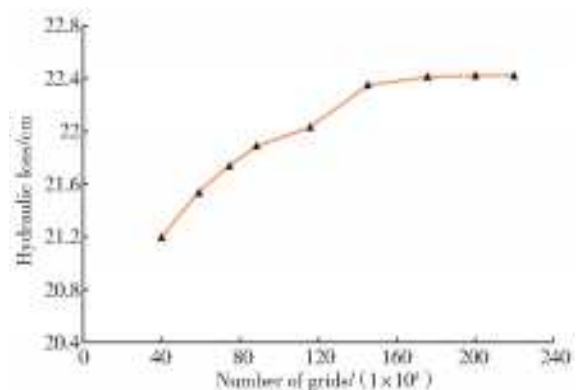


Fig. 3 Hydraulic loss under different grid numbers

3 Scheme optimization

3.1 Calculation scheme

The water flows into the forebay through the slope in the form of gate hole inflow. Due to the fast flow velocity of the water entering the forebay, the main flow area is mainly concentrated in the middle of the forebay, so the water can not be evenly diffused into each pump unit in a short period of time, and at the same time, a large return area is easily formed on both sides of the forebay, which is not conducive to the safe and stable operation of the pump unit. According to the design drawing of intake pumping station in a new water source area, a 3D model of pre-sedimentation aeration tank is established. The original scheme model is shown in Fig. 4. In view of the problems of flow separation and dead water area in the pre-sedimentation aeration tank, the fillet is used to optimize the original flow right angle in the pre-sedimentation aeration tank, and U-shaped diversion wall and quarter arc guide wall were added to the corridor. In view of the problem of flow deviation and backflow in the slope section, the splayed diversion wall is set in the forebay of the original scheme, and diversion piers are added between the pump units, so that the water can enter the forebay relatively smoothly. The 3D model of the improved scheme is shown in Fig. 5.

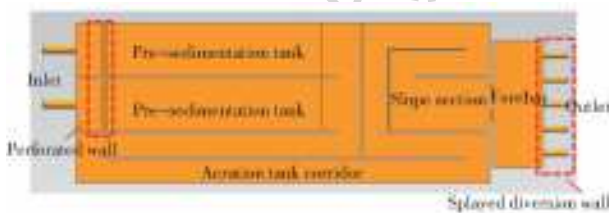


Fig. 4 Original scheme model

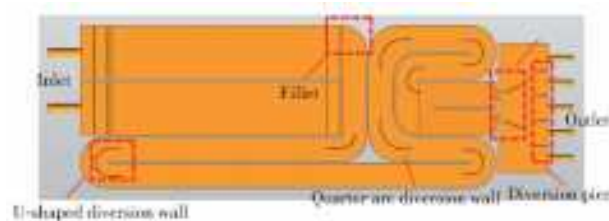


Fig. 5 Improved scheme model

3.2 Calculation results

In order to analyze the hydraulic characteristics of the intake pumping station under different

water level and flow rates of different schemes, the internal flow characteristics of different water intake pumping station schemes under two special working points (small flow $Q=7.80 \text{ m}^3/\text{s}$, large flow $Q=13.31 \text{ m}^3/\text{s}$) and three special water levels (design low water level 2.4 m, design constant water level 3.9 m, design high water level 6.8 m) were simulated. The section with a height of 1 m ($z=1 \text{ m}$) in the intake pumping station was selected as the analysis section, and the streamline diagram, flow velocity contour and pressure contour of the intake pumping station were obtained for comparative analysis.

3.2.1 Streamlines of intake pumping station

As shown in Fig. 6 to 8, by comparing the streamlines of the original scheme and the improved scheme under different flow rate and water level conditions, it can be seen that the flow pattern in the pre-sedimentation tank of the original scheme is relatively smooth, but there is a reflux area and disordered flow pattern at the corner of the corridor, and there is a large area of vortex and return area on the left side of the forebay. In the improved scheme, the problem of flow separation and reflux at the corner of corridor is improved, and the streamline distribution is more uniform. Under the condition of low water level, the large reflux area at the left side of forebay of the improved scheme can be eliminated, and the problem of poor flow pattern can be alleviated. Under the condition of constant water level and high water level, although there are vortices in the forebay of the improved scheme, the phenomenon of flow separation and reflux flow in the corridor and slope section is improved.

When the water level of the intake pumping station is constant, with the increase of flow rate, the change of streamlines of the two schemes is small, so the change of streamlines between the original scheme and the improved scheme is less affected by the change of flow rate.

When the flow rate is constant and the water level rises from low water level to constant and high water level, the overall flow pattern of the two schemes changes less than that of the low water level,

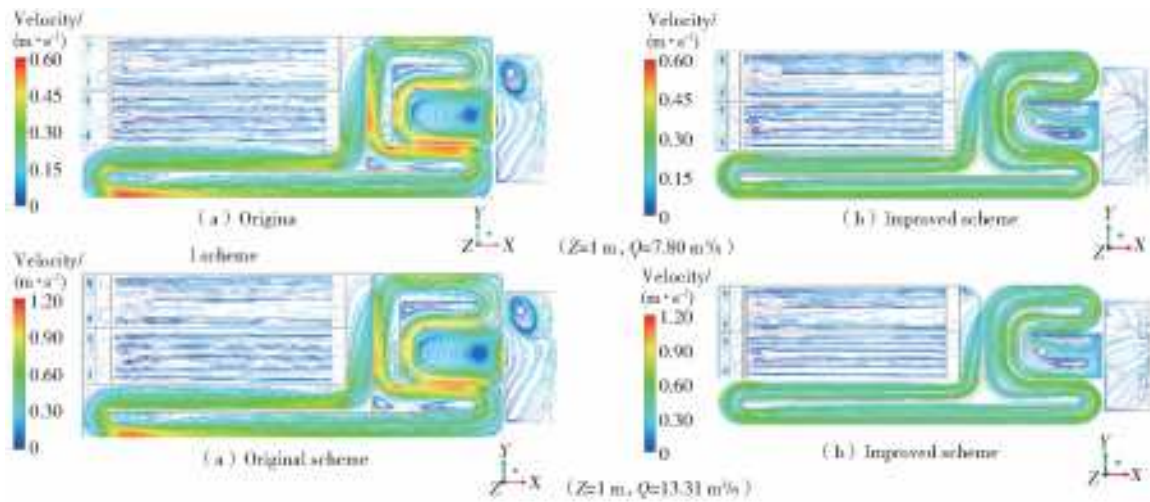


Fig. 6 Streamline diagrams of original and improved schemes under different flow conditions at low water level

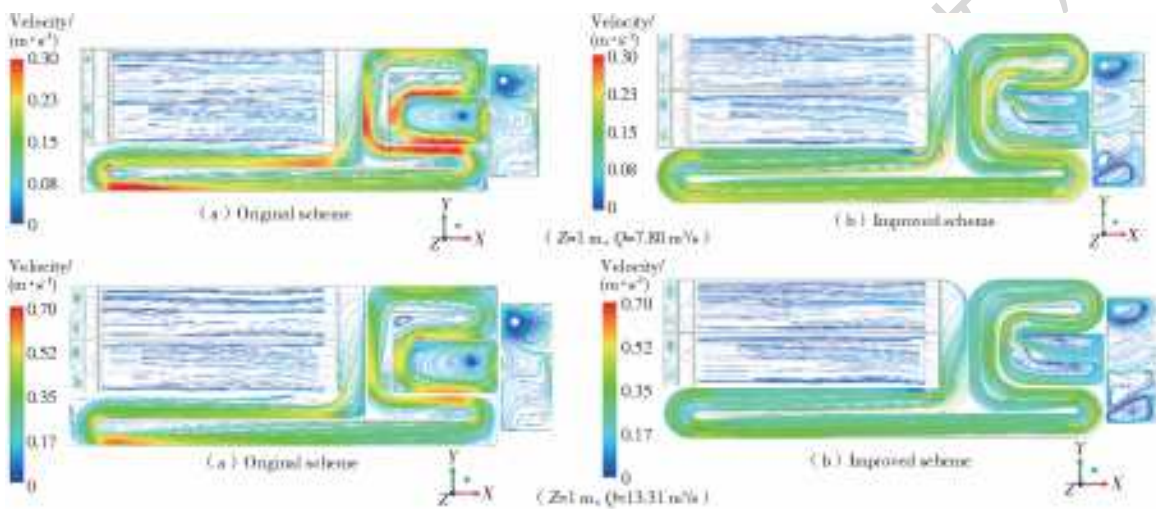


Fig. 7 Streamline diagrams of original and improved schemes under different flow conditions at constant water level

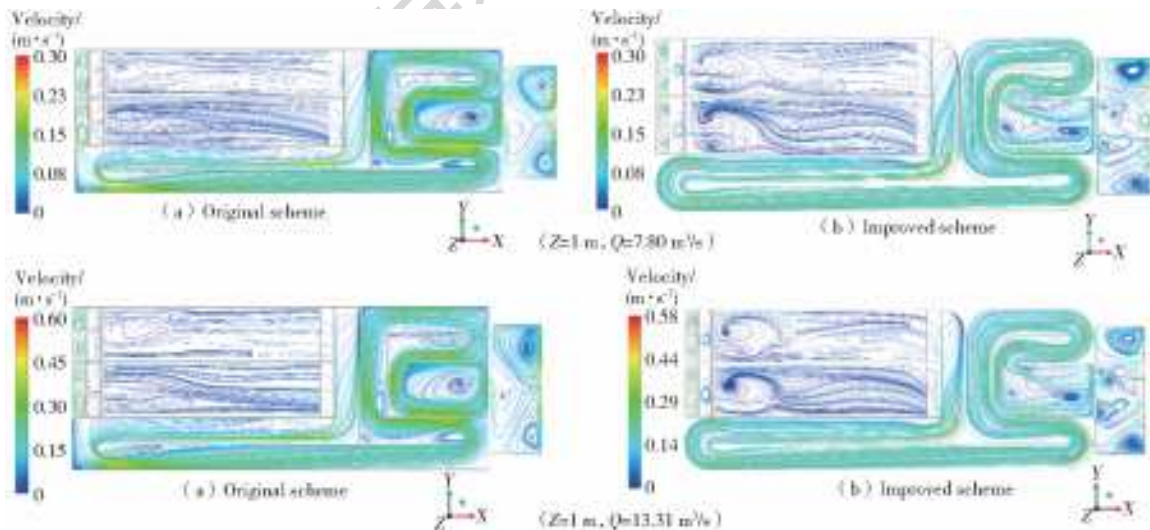


Fig. 8 Streamline diagrams of original and improved schemes under different flow conditions at high water level

and the improved scheme improves the poor flow pattern of the original scheme obviously.

3.2.2 Velocity contour of intake pumping station in different schemes

As shown in Fig. 9 to 11, by comparing the velocity contours of the original scheme and the im-

proved scheme under different flow rate and water level conditions, it can be seen that there is a high-speed area at the corner of the corridor of the original scheme, and the velocity distribution at the corner of the corridor is uneven. At the same time, the velocity distribution in the forebay is not uniform.

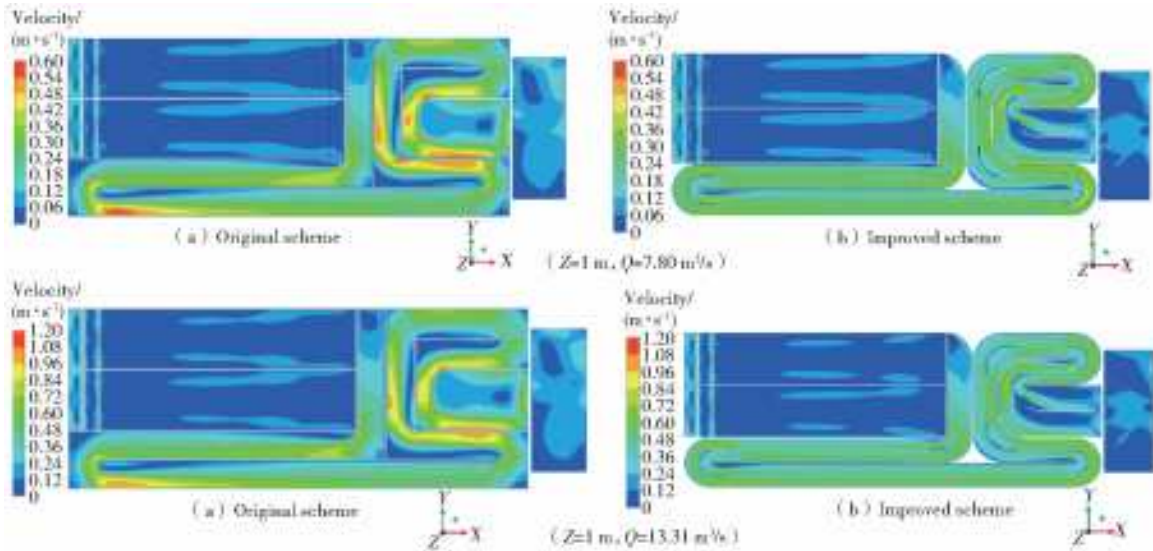


Fig. 9 Velocity contour of original and improved schemes under different flow conditions at low water level

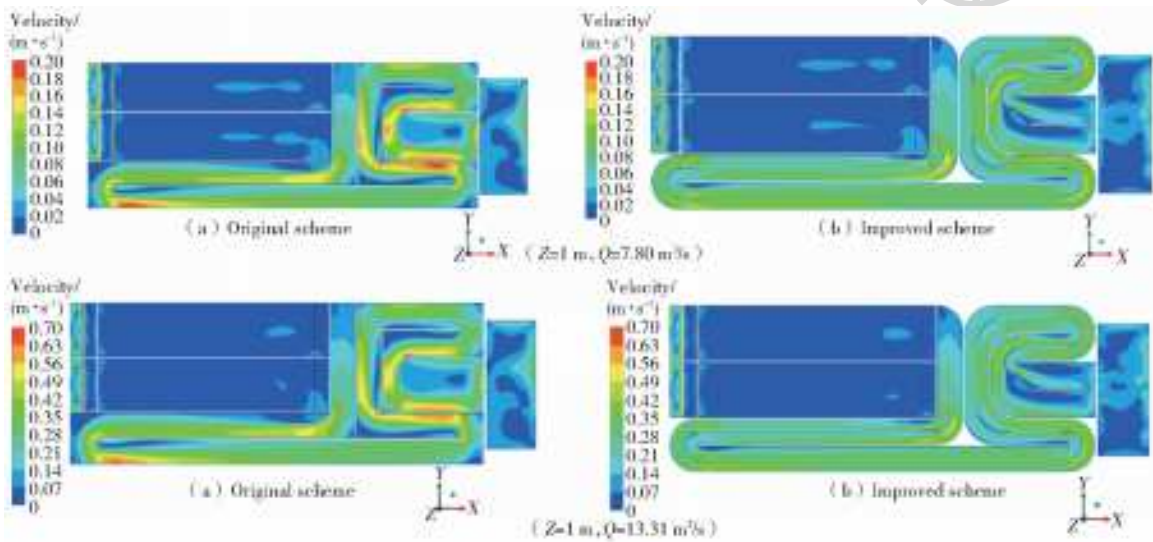


Fig. 10 Velocity contour of original and improved schemes under different flow conditions at constant water level

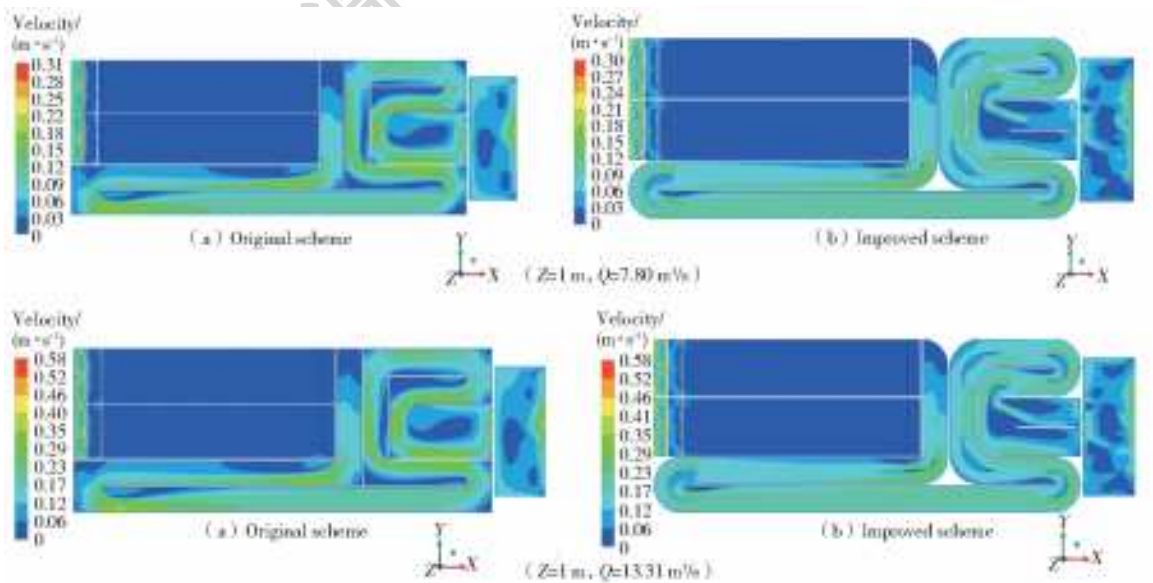


Fig. 11 Velocity contour of original and improved schemes under different flow conditions at high water level

In the improved scheme, the overall flow velocity distribution is more uniform, there is no obvious velocity fluctuation, and the flow velocity distribu-

tion at the corner of the corridor is improved. The overall flow velocity distribution of the improved scheme is relatively uniform. There is no obvious

velocity fluctuation in the improved scheme, and the uneven velocity distribution at the corner of the corridor is improved.

When the water level of the intake pumping station is constant, with the increase of flow rate, the overall velocity of the original scheme and the improved scheme increases gradually, but the variation law is similar. The change of velocity between the original scheme and the improved scheme is less affected by the flow.

When the flow rate is constant and the water level rises from low water level to constant and high water level, according to the velocity contour, the velocity of the two schemes of constant water

level and high water level is smaller than that of low water level, and the velocity distribution is basically unchanged. The improved scheme is beneficial to the uniform distribution of the overall velocity of the water intake pump station.

3. 2. 3 Pressure contour of intake pumping station in different schemes

As shown in Fig. 12 to 14, by comparing the pressure contours of the original scheme and the improved scheme under different flow rate and water level conditions, it can be seen that the pressure at the corner of the corridor of the improved scheme is smaller and the pressure distribution is more uniform than that of the original scheme.

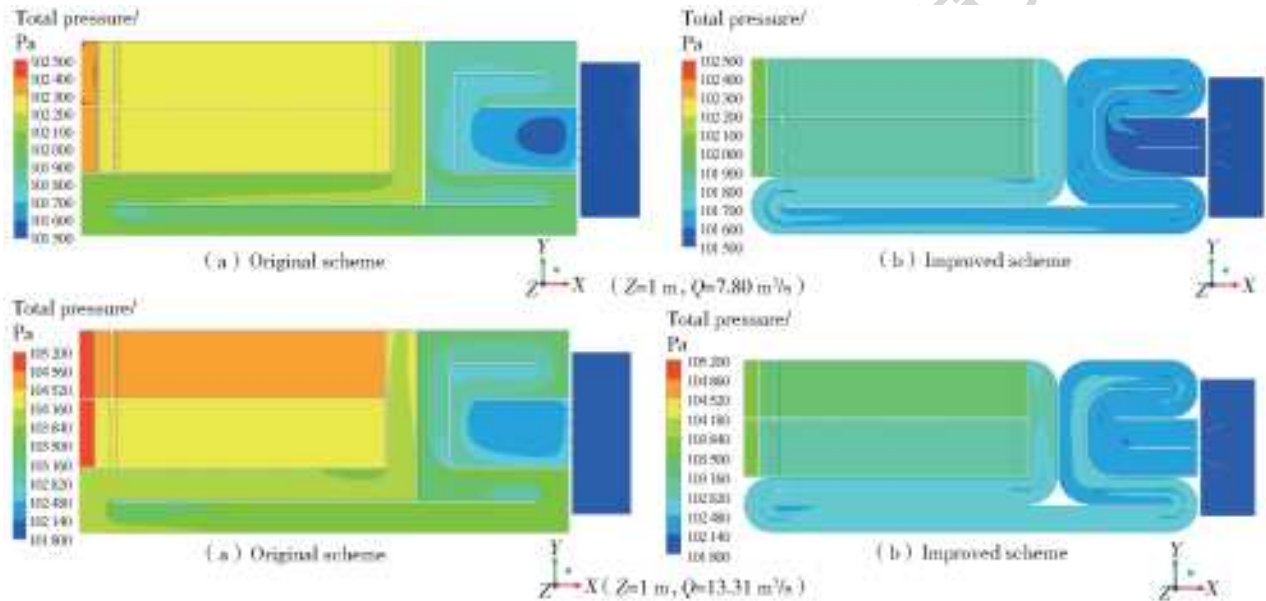


Fig. 12 Pressure contour of original and improved schemes under different flow conditions at low water level

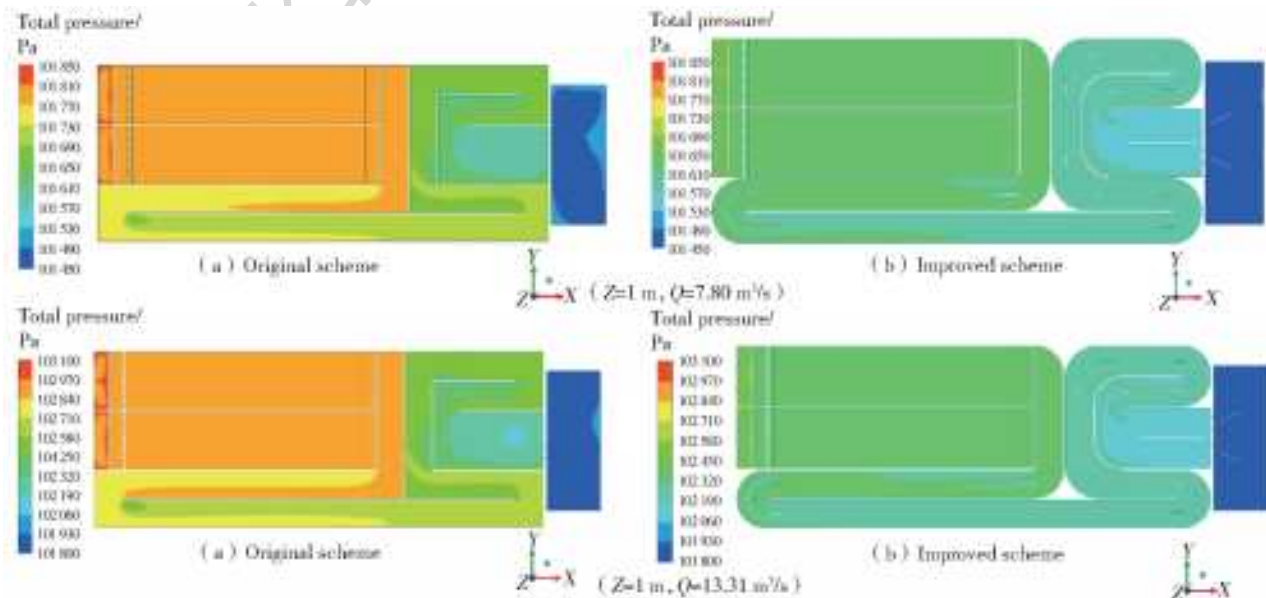


Fig. 13 Pressure contour of original and improved schemes under different flow conditions at constant water level

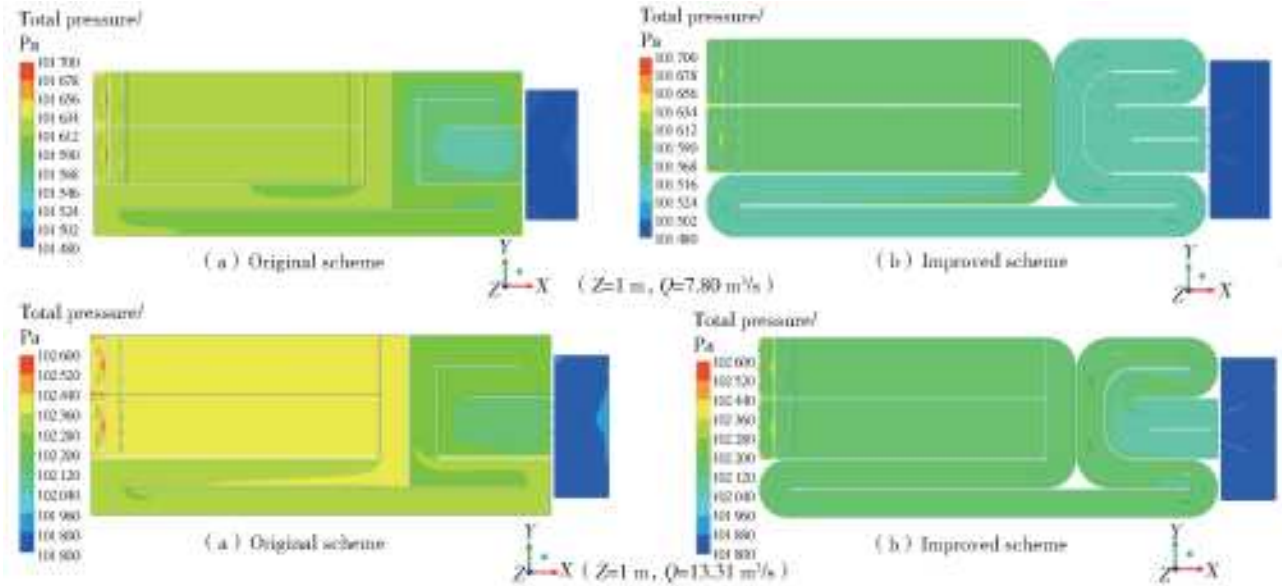


Fig. 14 Pressure contour of original and improved schemes under different flow conditions at high water level

When the water level of the intake pumping station is constant, with the increase of flow rate, the overall pressure in the original scheme and the improved scheme increases gradually, but the change rule is similar. The change of pressure distribution between the original scheme and the improved scheme is less affected by the flow.

When the flow rate is constant and the water level rises from low water level to constant and high water level, compared with the low water level, the overall pressure value of the improved scheme and the original scheme is reduced under the condition of high water

level and constant water level, but the pressure distribution is roughly the same, and the uniformity of the pressure distribution of the improved scheme is better than the original scheme.

3.3 Axial velocity distribution

In order to quantitatively analyze and compare the difference of water absorption uniformity between the original scheme and the improved scheme under the condition of large flow rate and small flow rate, the axial velocity distribution coefficient at the inlet section of the bell pipe of five pump units (Fig. 15) was compared and analyzed.

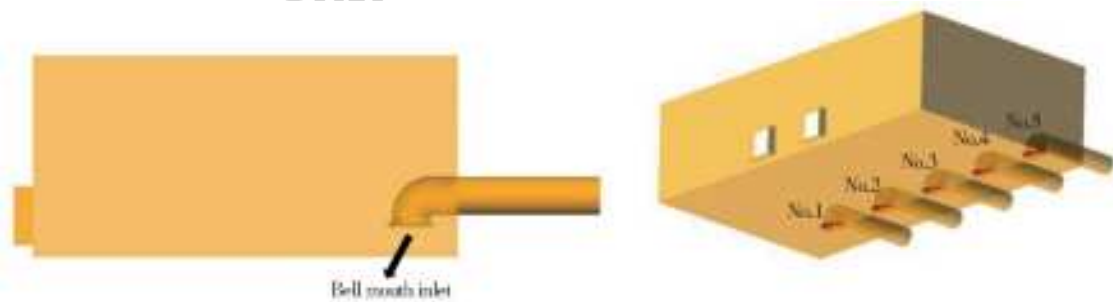


Fig. 15 Flow velocity uniformity of each inlet section of horn tube under different flow conditions

The formula for the axial velocity distribution coefficient \bar{V}_u is as follows:

$$\bar{V}_u = \left[1 - \frac{1}{u_a} \sqrt{\frac{\sum (u_{ai} - \bar{u}_a)^2}{m}} \right] \times 100\%$$

\bar{u}_a is the averaged axial velocity of the calculated section (m/s); u_{ai} is the axial velocity of each element of the calculated section (m/s); m is the number of cells of the calculated section.

Fig. 16 shows the axial velocity distribution coef-

ficient of each inlet section of the bell pipe under two flow rate conditions. The results show that under the condition of large flow rate and small flow rate, the uniformity of water absorption of each pump in the forebay without improvement measures is quite different, and the uniformity of water absorption of the pumps on both sides is poor. After the improvement measures are added, the axial velocity distribution coefficients of 5 pump units under two flow rate conditions are signif-

icantly improved, and the maximum increase range of the flow uniformity at the inlet section of the bell pipe is 3.6%, and the difference of the maximum flow uniformity at the inlet section of the bell pipe of each

pump unit is reduced to within 1.8%, but the water absorption uniformity of the pump units near the forebay is worse than that of the middle units.

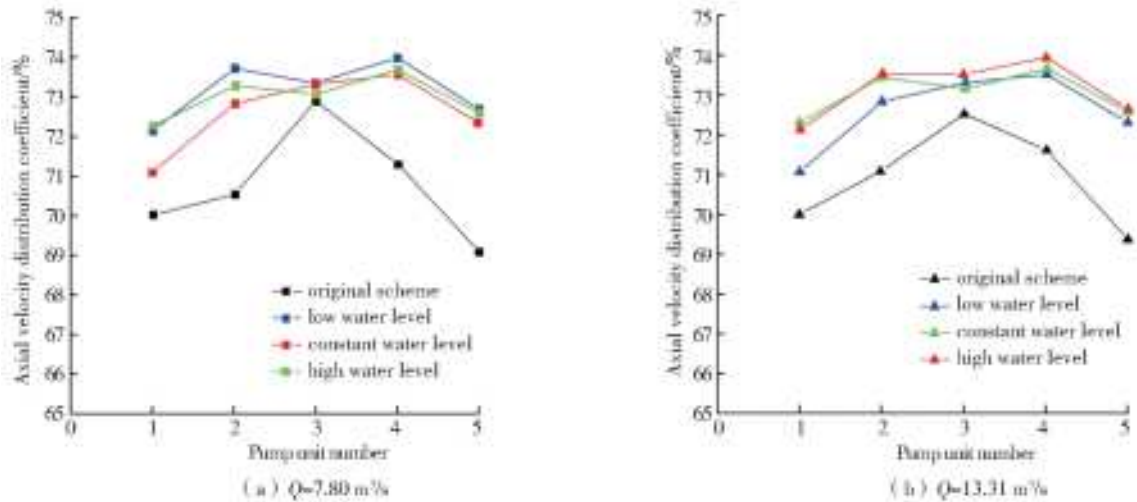


Fig. 16 Flow velocity uniformity of each inlet section of horn tube under different flow conditions

4 Conclusion

(1) Based on the original scheme, the following improvement measures are added to the improved scheme of intake pumping station: Fillets are set at the corner of the corridor of the aeration tank, U-shaped diversion wall and quarter arc-shaped diversion wall are set at the corner of the corridor, splayed diversion piers are set in the forebay and partition piers are set between the pump units. In the original scheme, the flow pattern in the sedimentation tank is relatively smooth, but there is reflux at the corner of the corridor, and the flow pattern is relatively disordered. In the original scheme, there was a large area of vortex and reflux area on the left side of the forebay. In the improved scheme, the flow separation and reflux at the corner of the corridor are improved, the streamline distribution is more uniform, and the uniformity of flow velocity at each inlet section of the bell pipe is greatly improved. Especially under the condition of low water level, the large reflux area on the left side of forebay can be eliminated, and there is no obvious adverse flow pattern in the forebay.

(2) When there is no improved measure in the forebay of the intake pumping station, the back wall will be impacted by the jet flow after the inlet of the slope gate hole, which is easy to form a large area of reflux area on both sides. A large area of reflux on the surface under the condition of low water level is well

controlled by setting a splayed diversion pier at the middle line of two sluice holes in the forebay and a partition pier between pump units.

(3) When the water level of the intake pumping station is constant, with the increase of flow rate, the flow pattern of the pre-sedimentation tank changes little, and the overall flow rate and pressure gradually increase, but the change rule is similar. When the flow rate is constant and the water level rises, the overall water flow pattern under high water level and constant water level conditions changes less than that under low water level condition. Obviously, the water suction uniformity of the water pump is significantly improved. In the improved scheme, the improvement measures are obvious to improve the poor flow pattern existing in the original scheme, and the uniformity of water absorption of the pump is significantly improved.

References:

- [1] LIU C. Pump and pumping station[M]. Beijing: China Water & Power Press, 2009.
- [2] CHENG L, LIU C, YAN H Q, et al. Flow characteristics and hydraulic performance of pumping stations [M]. Beijing: China Water & Power Press, 2016.
- [3] LI H, HUANG W, LIU T, PENG Z M. Discussion on ecological compensation mechanism for inter-basin water transfer[J]. Journal of Natural Resources, 2011, 26 (9): 1506-1512. (in Chinese) DOI: 10. 11849/zrzyxb. 2011. 09. 006.

- [4] ZHU W, TIAN B Y, LI C. Simulation and optimization of flow field distribution in pre-settling pool of Xihe water source area in South-to-North Water Transfer Project[J]. *China Water & Wastewater*, 2014, 30(9): 63-65. (in Chinese)
- [5] WANG J S, WANG Z Q. Study on process design of swirling pre-settling tank in Baotou City Shuikou water plant[J]. *Inner Mongolia Science technology & Economy*, 2005(1): 94-95. (in Chinese) DOI: 10. 3969/j. issn. 1007-6921. 2005. 01. 040.
- [6] WEI W L, ZHANG P, LIU Y L. Three-dimensional numerical simulation of hydraulic characteristics of advection sedimentation tank[J]. *Journal of Shenyang Agricultural University*, 2014, 45(4): 499-502. (in Chinese) DOI: 10. 3969/j. issn. 1000-1700. 2014. 04. 023.
- [7] BAI Y H, LI L, LIU T, et al. Study on the influence of wind speed and wind direction on flow movement in advection sedimentation tank based on LDV velocity measurement[J]. *Southwest Water & Wastewater*, 2014, 36(4): 14-20. (in Chinese)
- [8] LIU T J, HU R L, SUN Z, et al. Numerical simulation of inlet water and separator of advection wall in advection sedimentation tank[J]. *Water Technology*, 2015, 9(4): 1-6. (in Chinese) DOI: 10. 3969/j. issn. 1673-9353. 2015. 04. 001.
- [9] WANG X L, YANG L L, ZHANG M X, et al. Three-dimensional CFD simulation of flow in advection sedimentation tank[J]. *Journal of Tianjin University*, 2007(8): 921-930. (in Chinese) DOI: 10. 3969/j. issn. 0493-2137. 2007. 08. 008.
- [10] SU J W, WANG L, CHEN J. Summary and comments on numerical simulation study of secondary settling tank[J]. *Chinese Journal of Environmental Engineering*, 2019, 37(4): 87-92. (in Chinese) DOI: 10. 13205/j. hjgc. 201904017.
- [11] XIAO B Q, ZHANG F X, RONG G W. Influence of bubble size on numerical simulation of gas-liquid two-phase flow in aeration tank[J]. *China Environmental Science*, 2012, 32(11): 2006-2010. (in Chinese) DOI: 10. 3969/j. issn. 1000-6923. 2012. 11. 012.
- [12] LIU Y L, BAI G, SHAO S P, et al. Numerical simulation of influence of aeration pipe arrangement on flow rate distribution[J]. *Journal of Hydroelectric Engineering*, 2016, 35(7): 84-90. (in Chinese) DOI: 10. 11660/slfdx. 20160709.
- [13] CHENG W, SONG C, ZHOU X D, et al. Experimental study and numerical model of gas-liquid two-phase flow in aeration tank[J]. *Journal of Hydraulic Engineering*, 2001, 44(12): 42-45. (in Chinese). DOI: 10. 3321/j. issn: 0559-9350. 2001. 12. 006
- [14] WANG M, SUN N, WANG Y, CHENG W, et al. Experimental research and numerical simulation on gas-liquid two-phase flow of bubble velocity distribution in aeration tank[J]. *Journal of Hydraulic Engineering*, 2016, 47(10): 1322-1331. (in Chinese) DOI: 10. 13243/j. cnki. slxb. 20160530.
- [15] LUO C, CHENG L, LIU C. Numerical simulation of rectification mechanism of tank bottom before pumping station forward[J]. *Drainage and Irrigation Machinery*, 2014, 32(5): 393-398. (in Chinese) DOI: 10. 3969/j. issn. 1674-8530. 13. 0122.
- [16] GAO C J, LIU X Y, SHI L W, et al. Numerical simulation of rectification scheme for pumping station front pool and inlet pool[J]. *Journal of Hydroelectric Engineering*, 2011, 30(2): 54-59. (in Chinese)
- [17] GAO C J, WANG Y C, SHI L W, et al. Technical measures for non-continuous picking and dissipating energy in the front pool of pumping station[J]. *Drainage and Irrigation Machinery*, 2011, 29(2): 133-138. (in Chinese) DOI: 10. 3969/j. issn. 1674-8530. 2011. 02. 009.
- [18] CHENG L, LIU C, ZHOU J R, et al. Numerical simulation of two-dimensional turbulent flow around the bottom of pump station[J]. *Transactions of the Chinese Society for Agricultural Machinery*, 2005(3): 37-39. (in Chinese) DOI: 10. 3969/j. issn. 1000-1298. 2005. 03. 011.
- [19] CHENG L, LIU C, ZHOU J R, et al. Numerical simulation study on rectification of pumping station front bottom dam[J]. *Journal of Hohai University(Natural Sciences)*, 2001(3): 42-45. (in Chinese) DOI: 10. 3321/j. issn: 1000-1980. 2001. 03. 009.
- [20] FENG J G, LI J. Experimental study on flow pattern and improvement measures of front pool of large-scale urban water source pumping station[J]. *Advances in Science and Technology of Water resources*, 2010, 30(2): 70-74. (in Chinese) DOI: 10. 3880/j. issn. 1006-7647. 2010. 02. 018.
- [21] ZHOU L C. Numerical analysis of rectifier of the front pool pier of pumping station[J]. *Journal of Yangtze River Scientific Research Institute*, 2010, 27(2): 31-33. (in Chinese) DOI: 10. 3969/j. issn. 1001-5485. 2010. 02. 007.
- [22] YIN C. Three-dimensional numerical simulation study on flow state improvement of pumping station front pool[D]. Yangzhou: Yangzhou University, 2007. (in Chinese)
- [23] LIU C, CHENG L, TANG F P. Three-dimensional flow calculation and test of pumping station front pool[J]. *Transactions of the Chinese Society for Agricultural Machinery*, 2001(6): 41-44. (in Chinese) DOI: 10. 3969/j. issn. 1000-1298. 2001. 06. 012.
- [24] WANG F J. Research progress on calculation model of fluid mechanical rotating turbulence[J]. *Transactions of the Chinese Society for Agricultural Machinery*, 2016, 47(2): 1-14. (in Chinese) DOI: 10. 6041/j. issn. 1000-1298. 2016. 02. 001.
- [25] WANG W, ZHANG Y, CHEN L L. Construction and application of $k-\epsilon$ two-equation turbulence model with shear stress transport properties[J]. *Acta Aerodynamica Sinica*, 2019, 37(3): 419-425. (in Chinese) DOI: 10. 7638/kqdlxxb-2016. 0158.